Transcriptome Analysis of Human Diabetic Kidney Disease

Karolina I. Woroniecka,[1] Ae Seo Deok Park,[1] Davoud Mohtat,[2] David B. Thomas,[3] James M. Pullman,[4] and Katalin Susztak[1,5]

OBJECTIVE—Diabetic kidney disease (DKD) is the single leading cause of kidney failure in the U.S., for which a cure has not yet been found. The aim of our study was to provide an unbiased catalog of gene-expression changes in human diabetic kidney biopsy samples.

RESEARCH DESIGN AND METHODS—Affymetrix expression arrays were used to identify differentially regulated transcripts in 44 microdissected human kidney samples. DKD samples were significant for their racial diversity and decreased glomerular filtration rate (~25–35 mL/min). Stringent statistical analysis, using the Benjamini-Hochberg corrected two-tailed *t* test, was used to identify differentially expressed transcripts in control and diseased glomeruli and tubuli. Two different web-based algorithms were used to define differentially regulated pathways.

RESULTS—We identified 1,700 differentially expressed probesets in DKD glomeruli and 1,831 in diabetic tubuli, and 330 probesets were commonly differentially expressed in both compartments. Pathway analysis highlighted the regulation of Ras homolog gene family member A, Cdc42, integrin, integrin-linked kinase, and vascular endothelial growth factor signaling in DKD glomeruli. The tubulointerstitial compartment showed strong enrichment for inflammation-related pathways. The canonical complement signaling pathway was determined to be statistically differentially regulated in both DKD glomeruli and tubuli and was associated with increased glomerulosclerosis even in a different set of DKD samples.

CONCLUSIONS—Our studies have cataloged gene-expression regulation and identified multiple novel genes and pathways that may play a role in the pathogenesis of DKD or could serve as biomarkers. ***Diabetes*** **60:2354–2369, 2011**

Diabetes accounts for ~44% of patients starting treatment for kidney failure each year, including dialysis and renal transplantation (1,2). There are multiple representative changes on the renal biopsy that characterize diabetic nephropathy of humans (3). The earliest lesions are distinguished only by the thickening of the glomerular basement membrane without clear light-microscopical findings. In more advanced cases, mild and then moderate mesangial expansion can be observed. In general, diabetic kidney disease (DKD) is considered a nonimmune-mediated degenerative disease of the glomerulus; however, it has long been noted that complement and immunoglobulins sometimes can be detected in diseased glomeruli, although their role and significance is not clear (4).

The understanding of DKD has been challenged by multiple issues. First, the diagnosis of DKD is usually made using clinical criteria, and kidney biopsy often is not performed. According to current clinical practice, the development of albuminuria in patients with diabetes is sufficient to make the diagnosis of DKD (5). We do not understand the correlation between histological changes and the clinical phenotype. In addition, disease progression is variable; some patients progress relatively fast, whereas others do not, which could indicate a potentially heterogeneous disease (6,7). Twin studies highlighted the role of familiar associations in DKD; however, despite a large-scale and intense search, a causal mutation with a significant effect has not been identified (8,9). Another issue is the lack of mouse models that would faithfully recapitulate changes of human DKD (10). Most animal models show changes of early diabetic glomerulopathy, but they usually do not develop advanced changes, including diabetic glomerulosclerosis, advanced tubulointerstitial fibrosis, and renal function decline (11).

Genome-wide transcriptome analysis using expression arrays recently has gained popularity as a means to acquire insight into disease pathogenesis, molecular classification, and identification of biomarkers for progression or treatment response. The technology has been applied in the field of DKD as well; however, most gene-array studies have been performed on rodent diabetic models (12,13). Such murine-based experiments are limited because of the inherent differences between murine and human DKD. Few studies from the European Renal cDNA Bank have been published on microdissected human DKD kidney samples. To date, they only have focused on transcriptome analysis of the tubulointerstitial tissue from subjects with homogenous (Caucasian) backgrounds (14–18). These studies indicated the regulation of Janus kinase/signal transducer and activator of transcription (STAT), nuclear factor (NF) κB, and Wnt/β-catenin pathways.

The aim of our study was to provide an unbiased comprehensive catalog of gene-expression changes in human diabetic kidney biopsy samples. Here, we present a gene-expression analysis of 22 microdissected human renal glomerular and 22 tubule samples from healthy patients and patients with DKD from an ethnically diverse population. Our analysis has confirmed the regulation of multiple known pathways and highlighted the expression of many novel pathways in diabetic glomeruli. This study will aid the understanding of diabetic glomerular disease and could provide the basis for DKD biomarker discovery.

From the [1]Department of Medicine, Division of Nephrology, Albert Einstein College of Medicine, Bronx, New York; the [2]Department of Pediatrics, Division of Nephrology, Albert Einstein College of Medicine, Bronx, New York; [3]Nephrocor, Uniondale, New York; the [4]Department of Pathology, Albert Einstein College of Medicine, Bronx, New York; and the [5]Department of Genetics, Albert Einstein College of Medicine, Bronx, New York.

Corresponding author: Katalin Susztak, katalin.susztak@einstein.yu.edu.

Received 23 August 2010 and accepted 21 May 2011.

DOI: 10.2337/db10-1181

This article contains Supplementary Data online at http://diabetes.diabetesjournals.org/lookup/suppl/doi:10.2337/db10-1181/-/DC1.

K.I.W. and A.S.D.P. contributed equally to this study.

TABLE 1
Patient demographics

	Glomerular samples			Tubular samples		
	Control	DKD	*P*	Control	DKD	*P*
n	13	9		12	10	
Sex (female)	5	5		6	8	
Age (years)	51.38 ± 12.01	64 ± 13.56	3.2E–02	54.08 ± 13.81	63.5 ± 15.64	0.149
Ethnicity						
Asian Pacific Islander	0	0		1	0	
Non-Hispanic white	6	2		3	3	
Non-Hispanic black	3	3		4	6	
Hispanic	3	4		2	1	
Other and unknown	1	0		2	0	
BMI (kg/m^2)	29.59 ± 9.08	32.74 ± 7.9	0.41	28.60 ± 5.65	32.87 ± 8.31	0.169
Hypertension	4	9		6	8	
Diabetes	0	9		0	10	
Proteinuria (dipstick)	0.69 ± 0.85	2.55 ± 1.74	3.0E–03	0.4 ± 0.84	3.4 ± 0.84	2.65E–07
Spot protein (mg/dL)*	0.45 ± 0.17	1.97 ± 0.78	9.1E–03	0.86 ± 0.69	2.41 ± 0.67	8.1E–03
Spot creatinine (mg/dL)*	1.76 ± 0.21	1.79 ± 0.13	0.823	1.83 ± 0.18	1.69 ± 0.11	0.213
Spot PCR*	−1.31 ± 0.12	0.41 ± 0.89	6.9E–03	−0.57 ± 1.15	0.94 ± 0.61	4.0E–02
Hematuria	0.07 ± 0.27	0.66 ± 0.86	3.1E–02	0.0 ± 0.0	0.8 ± 1.22	0.054
Serum creatinine (mg/dL)	1.02 ± 0.24	2.83 ± 1.55	4.7E–04	1.06 ± 0.21	3.39 ± 1.60	7.04E–05
Serum BUN (mg/dL)	13.53 ± 4.53	40.44 ± 22.65	4.3E–04	13.75 ± 4.26	37.9 ± 15.14	3.46E–05
eGFR (mL/min)	80.91 ± 23.42	31.08 ± 13.36	1.2E–05	73.77 ± 21.08	21.85 ± 11.54	9.55E–07
Histology						
Glomerulosclerosis (%)	0.32 ± 0.96	24.39 ± 13.20	4.3E–06	0.49 ± 1.00	33.80 ± 28.59	6.1E–04
Endothelial lumen: patent (%)	100 ± 0	93 ± 13.03	6.9E–02	99.54 ± 1.50	81.66 ± 20.41	9.4E–03
Lumen: cells	0	0		0	0	
Lumen: thrombi	0	0		0	0	
Mesangial cells	0 ± 0	0.75 ± 0.95	1.5E–02	0 ± 0	0.6 ± 0.54	3.1E–03
Increased mesangial matrix	0.16 ± 0.57	1.6 ± 1.5	1.0E–02	0.09 ± 0.30	2.16 ± 1.16	4.2E–05
Bowman's capsule thickening	0.0 ± 0.0	1.5 ± 1.29	3.4E–03	0.3 ± 0.48	1.8 ± 0.83	6.4E–0.4
Tubular atrophy (%)	2.5 ± 3.98	23.88 ± 13.64	5.2E–05	2.66 ± 5.78	35 ± 21.08	5.3E–05
Interstitial fibrosis (%)	2.08 ± 3.96	31.11 ± 26.19	1.1E–03	3.5 ± 4.33	39 ± 24.69	8.4E–05
Vascular sclerosis	0.7 ± 0.96	1.42 ± 0.78	0.1127	0.70 ± 0.86	1.62 ± 0.74	2.4E–02

Data are *n* or means ± SD. Demographics and histological analysis: eGFR was calculated using the Modification of Diet in Renal Disease formula. *Spot protein, creatinine, and PCR were $\log_{10}$ transformed. An arbitrary scale was used to evaluate dipstick proteinuria (0 = negative, 1 = trace, 2 = 30 mg/dL, 3 = 100 mg/dL, and 4 = 300 mg/dL) as well as hematuria (0 = red blood cell count <5, 1 = red blood cell count 6–20, 2 = red blood cell count 21–50, 3 = red blood cell count >50). Vascular sclerosis: 0 = normal; 1 = mild; 2 = moderate; and 3 = severe. Student *t* test was used to determine the statistical significance between groups for age, weight, BMI, proteinuria, serum creatinine, serum BUN, and eGFR. Lumen cells and lumen thrombi: 0 = normal and 1 = increased. Mesangial matrix: 0 = normal; 1 = focal; 2 = increased, mild; and 3 = increased, nodular. Bowman's capsule thickening: 0 = normal; 1 = focal; 2 = mild circumferential; 3 = moderate; and 4 = severe.

RESEARCH DESIGN AND METHODS

The clinical study used a cross-sectional design. Kidney samples were obtained from living allograft donors and surgical nephrectomies and from leftover portions of diagnostic kidney biopsies. Nephrectomies were anonymized with the corresponding clinical information and were collected by an individual who was not involved in the research protocol. These samples were collected without consent. For protocol allograft and kidney biopsies, informed consent was obtained from the donor. The study was approved by the institutional review board of the Albert Einstein College of Medicine and Montefiore Medical Center (2002-202 to K.S.).

Tissue handling and microdissection. Tissue was placed into RNALater and manually microdissected at 4°C for glomerular and tubular compartment. In general, five glomeruli that readily released from the capsule were collected and placed into cold RNAeasy lysis buffer solution (Qiagen RNeasy kit). The corresponding tubulointerstitial and vascular compartment also was placed into RNAeasy lysis buffer solution. For easier designation, we refer to this component as tubules throughout the article. Dissected tissue was homogenized and RNA was prepared using RNAeasy mini columns (Qiagen, Valencia, CA), according to manufacturer's instructions. RNA quality and quantity were determined using the Laboratory-on-Chip Total RNA PicoKit Agilent BioAnalyzer. Only samples without evidence of degradation were further used.

Microarray procedure. For the human kidney tissue (glomeruli or tubuli), purified total RNAs were amplified using the Two-Cycle Target Labeling Kit (Affymetrix), as per the manufacturer's protocol (19). The raw and analyzed data files have been uploaded to the National Center for Biotechnology Information Gene Expression Omnibus and can be accessed under the following accession numbers: GSE 30122 (all data samples).

Bioinformatics. After hybridization and scanning, raw data files were imported into GeneSpring GX software (Agilent Technologies). Raw expression levels were normalized using the RMA16 summarization algorithm. This normalization method is a mathematical technique used to obtain variance stabilization and reduce discrepancies in hybridization patterns that might result from variables in target amplification, hybridization conditions, staining, or probe array lots. GeneSpring GX software then was used for statistical analysis. We used a Benjamini-Hochberg multiple-testing correction with a P value < 0.05.

Transcription factor binding sites. Enrichment of transcription factor binding sites (TFBSs) was determined using oPOSSUM software (20) for the identification of overrepresented TFBSs in coexpressed genes, which determines the overrepresentation of TFBSs within a set of coexpressed genes compared with a precompiled background set.

Pathway analysis. Differentially expressed transcripts satisfying the statistical conditions then were exported to Ingenuity Pathway Analysis software (Ingenuity Systems). This software determines the top canonical pathways by using a ratio (calculated by dividing the number of genes in a given pathway that meet cutoff criteria by the total number of genes that constitute that pathway) and then scoring the pathways using a Fischer exact test (P value < 0.05). The significance of the given pathway for the dataset is a measurement of the likelihood that the pathway is associated with the dataset by random chance. The Database for Annotation, Visualization, and Integrated Discovery bioinformatics package (21) also was used for pathway analysis and to provide gene ontology of the differentially expressed genes (22).

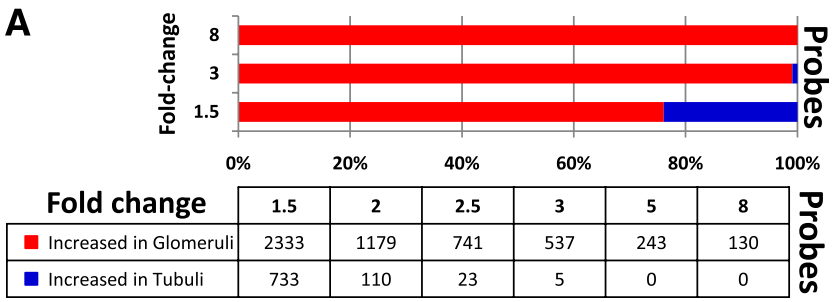

Fold change	1.5	2	2.5	3	5	8
Increased in Glomeruli	2333	1179	741	537	243	130
Increased in Tubuli	733	110	23	5	0	0

Probes

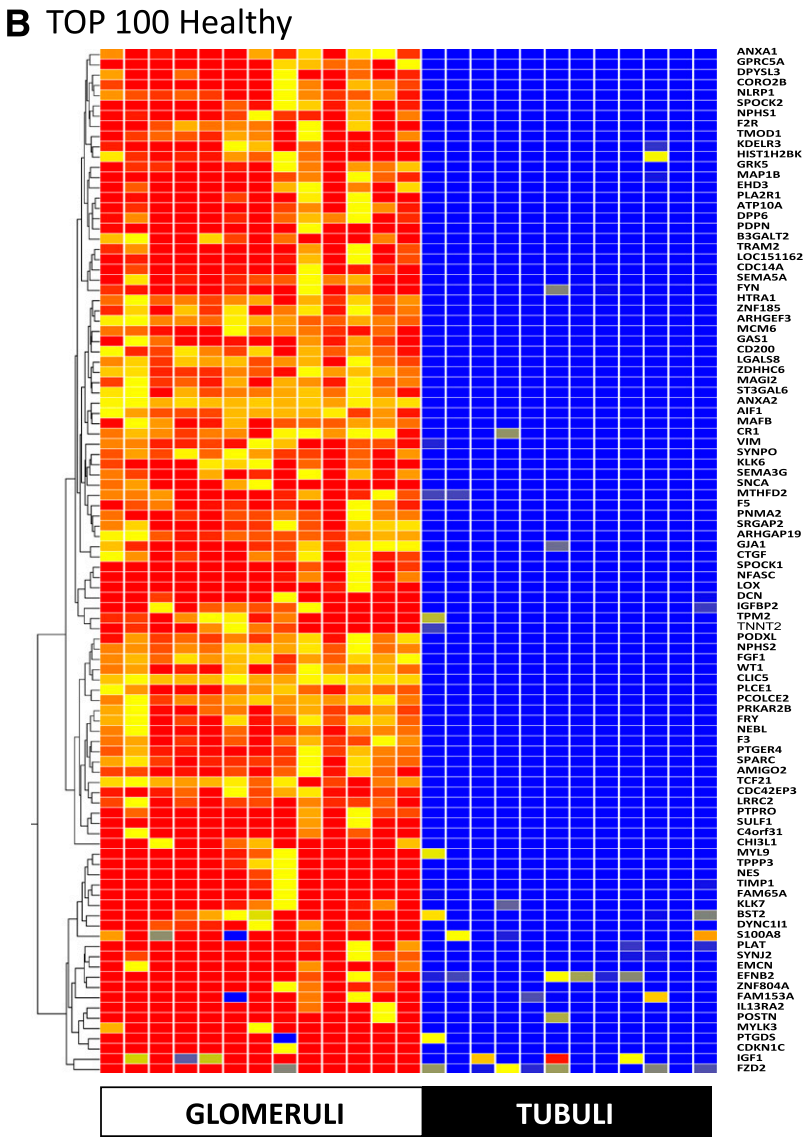

FIG. 1. Differentially expressed transcripts in healthy glomeruli compared with the tubulointerstitium. *A*: Statistical significance was determined using a fold-change cutoff of 1.5 and a Benjamini-Hochberg multiple-testing correction *P* value < 0.05. The graph represents the number of increased (red) or decreased (blue) probesets in the glomerular compartment with the indicated fold change (1.5- to 8.0-fold). *B*: Hierarchal cluster (Manhattan distance and complete linkage) of the 100 transcripts with highest fold change showing increased expression in glomeruli (i.e., glomerular specific). One row represents one gene and one column represents one sample. Blue color signifies downregulation and red color signifies upregulation.

Histology. Histology was evaluated using periodic acid-Schiff–stained kidney sections by two expert nephropathologists. Glomerular sclerosis, endothelial lumen, the presence of cells or thrombi, mesangial cells and matrix, Bowman's capsule, tubular atrophy, interstitial fibrosis, and vascular sclerosis were evaluated by two independent pathologists. The degree of sclerosis, thickening, and fibrosis was evaluated on the basis of an arbitrary scale and was taken from routine pathological evaluations. C3 and C1q immunofluorescence-staining results were obtained from routine evaluations of diabetic nephropathy cases.

Immunostaining. Immunostaining was performed as described earlier (19). We used the following primary antibodies: C3 (ab15981; Abcam); CLIC5 (ARP35263P100; Aviva Biosystems); and podocin (P0372; Sigma). We used the Vectastain ABC Elite kit for secondary antibodies and 3,3"diaminobenzidine for visualizations. After coding, the degree of glomerular immunostaining was

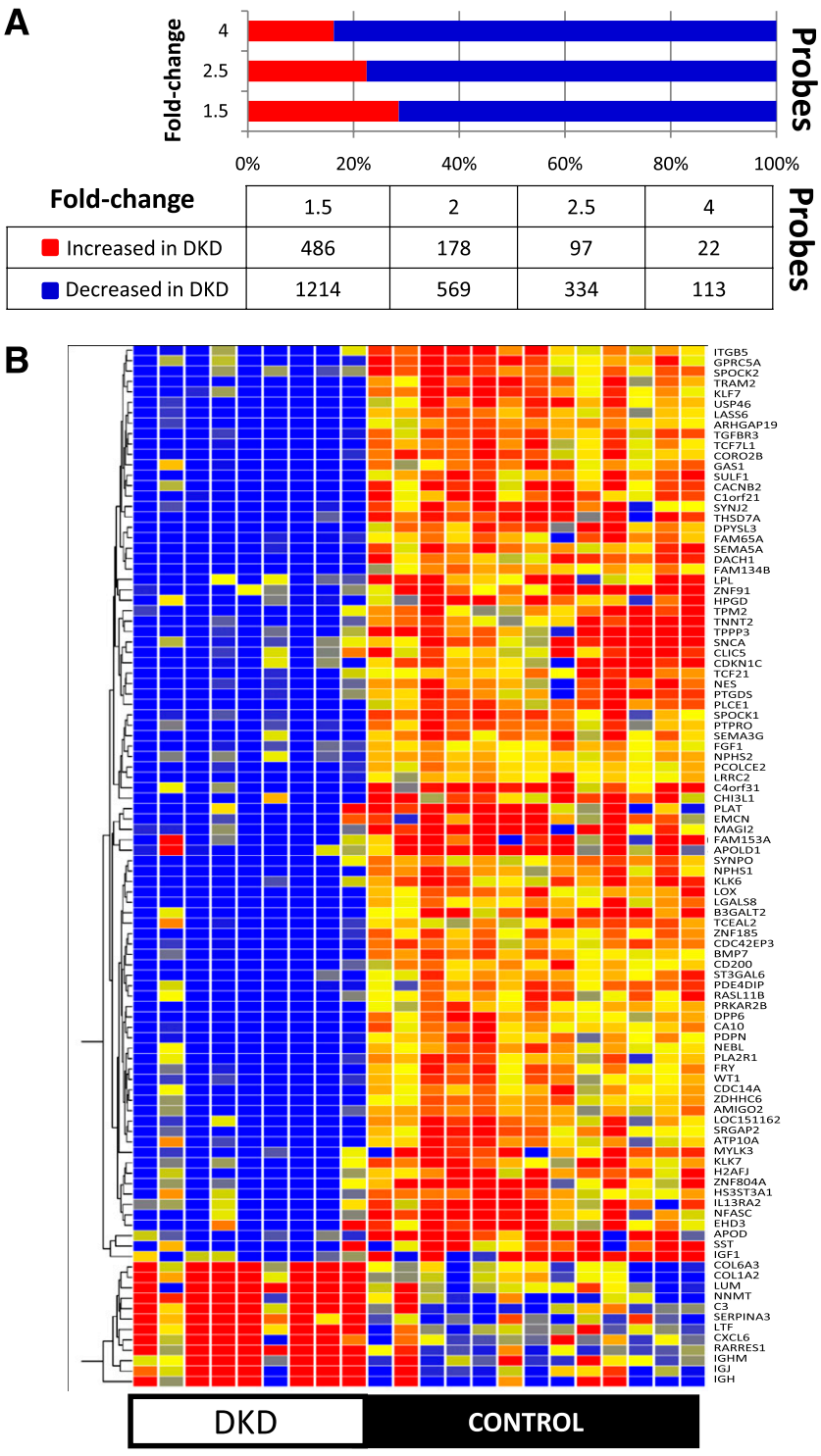

Fold-change	1.5	2	2.5	4
Increased in DKD	486	178	97	22
Decreased in DKD	1214	569	334	113

Probes

FIG. 2. Differentially expressed transcripts in DKD glomeruli. *A*: Statistical significance was determined using a fold-change cutoff of 1.5 and a Benjamini-Hochberg multiple-testing correction *P* value < 0.05. The graph represents the number of increased (red) or decreased (blue) probesets in the glomerular compartment with the indicated fold change (1.5- to 4.0-fold). *B*: Hierarchal cluster (Manhattan distance and complete linkage) of the 100 genes with highest fold change differentially expressed in control and DKD glomeruli.

scored on an arbitrary scale of 0–4 (0 = 0% stain, 1 = <25% stain, 2 = moderate 25–50% stain, 3 = 50–75% stain, and 4 = >75% stain).

RESULTS

Characteristics of the research participants. Twenty-two glomerular and 22 tubular kidney samples were collected from healthy, living transplant donors; nephrectomies; and diagnostic kidney biopsies. The research population was notable for its ethnic diversity. Tissue samples were categorized on the basis of the clinical evaluations (Table 1) and on the basis of histological readings of the kidney samples (Table 1). For the glomerular analysis, we chose 9 DKD and 13 control samples, whereas for the tubular analysis we chose 10 DKD and 12 control samples. Cases were notable for statistically significant decreased estimated glomerular filtration rates (eGFRs), increased proteinuria,

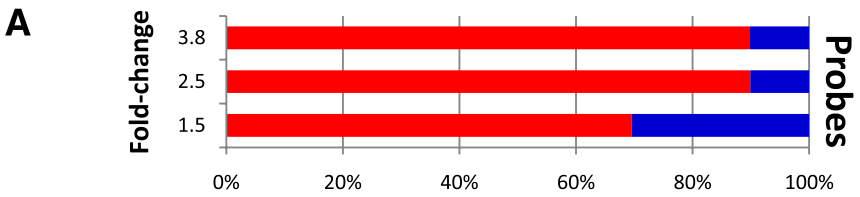

Fold-change	1.5	2	2.5	3.8
Increase in DKD	1273	653	347	115
Decrease in DKD	558	100	39	13

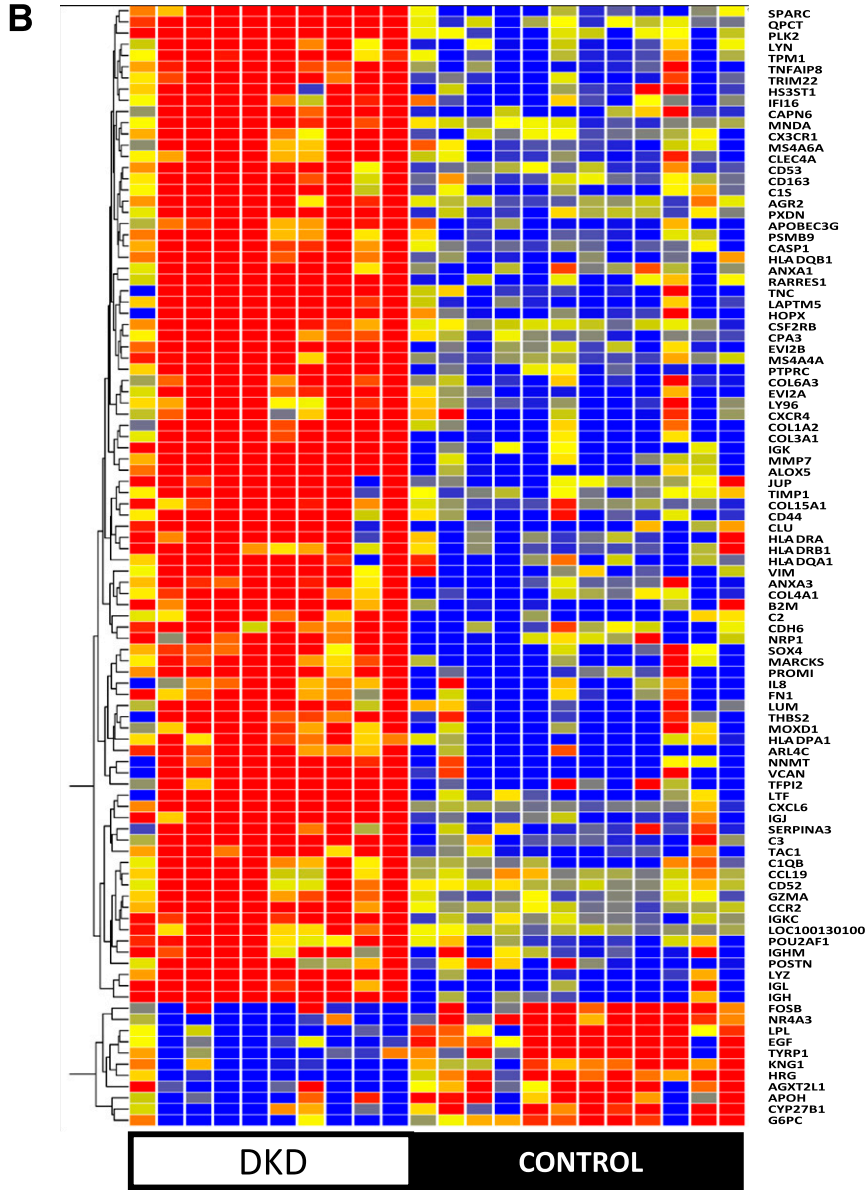

FIG. 3. Differentially expressed transcripts in DKD tubulointerstitium compared with control samples. *A*: Statistical significance was determined using a fold-change cutoff of 1.5 and a Benjamini-Hochberg multiple-testing correction *P* value < 0.05. The graph represents the number of increased (red) or decreased (blue) probesets in the glomerular compartment with the indicated fold change (1.5- to 3.8-fold). *B*: Hierarchal cluster (Manhattan distance and complete linkage) of the 100 transcripts with highest fold change differentially expressed in control and DKD tubulointerstitium.

serum creatinine, blood urea nitrogen (BUN), as well as the presence of hypertension. Histological evaluation showed statistically significantly increased glomerulosclerosis, tubular atrophy, interstitial fibrosis, vascular sclerosis, and mesangial matrix expansion. Representative glomerular images also are shown in Fig. 4. Cases were defined by the presence of diabetes, proteinuria, GFR <60 mL/min, histological changes consistent with DKD, and the absence

of hepatitis, HIV, lupus, or other potential causes of glomerulonephritis. Control samples were obtained from healthy, living transplant donors ($n = 6$ in the glomerular study and $n = 4$ in the tubular study) or biopsy samples of the unaffected portion of tumor nephrectomies. We could not detect differentially expressed probesets between glomeruli obtained from donor or tumor nephrectomies (data not shown). Control subjects were defined as having an eGFR >60 (mL/min), the absence of proteinuria, normal serum creatinine and BUN, and <10% glomerular and tubulointerstitial fibrosis. In summary, the phenotype analysis was significant for the racial diversity of the subjects and advanced chronic kidney disease (stage III-IV) in our cases.

Gene-expression differences between healthy glomerular and tubular human kidney tissue. The kidney tissue was microdissected into glomerular and tubulointerstitial fractions, as previously described (19), and Affymetrix U133 A2.0 expression arrays were performed separately on glomerular and tubular fractions. First, we compared 12 tubular samples with 13 glomerular samples isolated from control "healthy" kidneys. We used GeneSpring GX software to provide statistical analysis (t test with Benjamini-Hochberg multiple-testing correction, $P < 0.05$, and fold change >1.5). Such analysis defined 3,066 differentially expressed probesets between the tubular and glomerular tissue (Supplementary Table 1). Of 3,066 probesets, 243 probesets showed a fold change >5.0 between glomeruli and tubuli. All of these top differentially expressed probesets showed much higher expression in glomeruli compared with the tubulointerstitial compartment (i.e., their expression was glomeruli specific) (Fig. 1). The top 100 transcripts with the highest fold change are shown as a hierarchal cluster in Fig. 1*B*. Some of these highly differentially expressed transcripts may represent novel glomerular-specific genes, such as *ARHGAP19*, *TCF21*, *IL13RA2*, and *CH13L1*. Other transcripts are known to have prominent glomerular expression, such as *PLA2R*, *CLIC5*, *PLCE1*, *WT1*, *NPHS1*, *NPHS2*, *PODXL*, *SYNPO*, and *TJP1*. Five transcripts showed almost exclusive expression in tubulointerstitial tissue, with a fold change >3.0; as expected they were mainly solute carriers and channels (*SLC22A*, *SLC4A4*, *STC1*, *SFRP1*, and *KCNJ1*). This analysis validated the microdissection procedure and identified a compendium of glomerular-specific transcripts.

Gene-expression differences between healthy and diseased human kidney tissue. Next, we determined gene-expression differences in isolated control and DKD glomeruli using stringent statistical analysis (t test unpaired, Benjamini-Hochberg multiple-testing correction, $P < 0.05$, fold change >1.5). This analysis identified 1,700 differentially expressed probesets between control and case subjects. The majority of the probesets (1,214 [~70%]) showed decreased expression in DKD glomeruli (Fig. 2*A*) (Supplementary Table 2). The top 100 regulated genes showed a more than fourfold change shown in a hierarchal cluster format in Fig. 2*B*. Almost all podocyte-specific transcripts showed severe decreased expression, for example *PLCE1* (ninefold), *PTGDS* (sevenfold), *NPHS1* (eightfold), *NPHS2* (fivefold), *SYNPO* (sixfold), *PLA2R1* (sixfold), *WT1* (fivefold), *CLIC5* (fourfold), and *PODXL* (fourfold). The expression and regulation of podocyte-specific genes, *NPHS2* and *CLIC5*, were confirmed by immunohistochemistry as well. The protein and mRNA level data showed an excellent correlation (Supplementary Figs. S1 and S2). These studies are consistent with the key role that podocytes play in DKD development. Transcripts that showed the highest increase in their expression included *IGH* (14-fold), *C3* (6-fold), *COL1A2* (6-fold), *CXCL6* (5-fold), and *COL6A3* (4.6-fold). These transcripts are known to be associated with fibrosis and inflammation.

Next, we determined the gene-expression differences in control and DKD tubular tissue. We identified 1,831 differentially expressed probesets between control and diseased tubule tissue (Fig. 3) (Supplementary Table 3). Most transcripts showed increased expression in DKD tubuli because 1,273 probsets (~70%) showed increased expression and only 558 showed lower expression in DKD. The top differentially regulated genes in DKD tubuli included transcripts that are associated with inflammation and fibrosis, including *IGH* (31- to 46-fold change), *IGL* (17-fold change), multiple collagen transcripts *COL1A2* (4- to 7-fold change), and *COL3A1* (6-fold change). This comprehensive analysis of differentially expressed transcripts in DKD glomeruli and tubuli revealed the regulation of many novel transcripts and highlighted many of the known changes in fibrosis and immune-regulated transcripts.

Compartmental regulation of genes in DKD glomeruli and tubuli. Next, we were interested in determining the compartmental regulation of transcripts in diabetic kidneys. We identified 330 differentially regulated probesets common to tubular and glomerular tissue by comparing genes differentially expressed in control and DKD glomerular tissue (1,700 probesets) to those differentially expressed in tubulointerstitial tissue (1,831 probesets) (Supplementary Table 4). Of 330 commonly regulated probesets, 73% showed similar regulation in the glomeruli and tubuli; most of them ($n = 201$) were increased in both compartments, whereas 40 transcripts were decreased in both compartments. The remaining probesets ($n = 89$) were decreased in DKD glomeruli and increased in DKD tubuli (Supplementary Table 4). In summary, a small number of probesets ($n = 330$ [~19%]) showed differential regulation in both glomeruli and tubuli in diabetic kidneys, indicating important compartment-specific regulation.

Enrichment of TFBSs in DKD kidneys. To understand commonalities in the regulation of differentially expressed transcripts in healthy and DKD glomeruli, we examined the upstream TFBSs of these genes. Using the oPOSSUM bioinformatics toolset (20) (which compiles a background dataset from the Ensembl database and vertebrate), TFBSs within the 5-kb-upstream regions of the differentially expressed DKD genes were determined. The Fisher exact test (P value < 0.01) was used to determine significance. This analysis identified a total of 23 TFBSs (Supplementary Table 5). It is interesting to note that six of the *FOX* family TFBSs were identified, including *FOX-D1*, *-I1*, *-Q1*, *-F2*, *-D3*, and *-A2*. Other notable TFBSs included *STAT1* and *Cebpa*, which have been shown to be regulated in DKD. The differentially expressed genes showed enrichment for multiple TFBSs, and some of the top TFBSs showed correlation to previous studies.

Regulation of canonical pathways in DKD tubuli. To determine pathways differentially regulated in DKD tubuli, we used two different bioinformatics tools. The Ingenuity Pathway Analysis software determines top canonical pathways by using a ratio, calculated by dividing the number of genes in a given pathway that meet cutoff criteria by the total number of genes that constitute that pathway, and then scoring the pathways using the Fisher exact test (P value < 0.01). The Ingenuity Pathway Analysis showed 103 pathways of statistical significance. The top pathways

TABLE 2
Selected differentially expressed pathways in DKD tubuli

Canonical pathways	*P*	Ratio	Molecules
CTL-mediated apoptosis of target cells	1.20E–10	2.84E–01	B2M, HLA-DMA, CASP3, HLA-DQA1, APAF1, HLA-DRB1, HLA-DMB, CD3D, FAS, HLA-DPA1, HLA-F, HLA-DQB1, CASP6, CASP9, HLA-A, HLA-E, HLA-DRA, HLA-B, FCER1G, CASP8, HLA-G, HLA-DPB1, and HLA-C
Type 1 diabetes signaling	1.10E–09	3.06E–01	MAP2K4, JAK1, NFKBIE, HLA-DQA1, HLA-DRB1, HLA-DMB, JAK2, FAS, HLA-F, IKBKB, CD28, CASP9, HLA-A, HLA-DRA, HLA-B, STAT1, TNFRSF1B, HLA-G, CASP8, TNFRSF11B, HLA-C, HLA-DMA, CASP3, MYD88, APAF1, MAPK8, IFNGR1, IL1R1, CD3D, IRF1, HLA-DQB1, HLA-E, GAD1, FCER1G, MAP2K3, SOCS7, and SOCS5
Cdc42 signaling	3.80E–09	2.24E–01	B2M, MAP2K4, ARPC1B, ARPC5, HLA-DQA1, HLA-DRB1, HLA-DMB, IQGAP1, HLA-DPA1, HLA-F, ACTR3, HLA-A, BAIAP2, HLA-DRA, HLA-B, ARPC3, MYL10, HLA-G, HLA-DPB1, ITGA4, HLA-C, ITGB1, HLA-DMA, ACTR2, SRC, PAK4, PAK2, MYLPF, ITGA2, MAPK8, CD3D, HLA-DQB1, WIPF1, HLA-E, MYL12B, ARHGEF6, FCER1G, PPP1R12A, and VAV1
Role of macrophages, fibroblasts, and endothelial cells in rheumatoid arthritis	1.00E–08	1.93E–01	MAP2K4, TLR1, TRAF3, WNT10B, PRSS2, CSNK1A1, LTB, PLCH2, MYC, VEGFA, IKBKB, TRAF3IP2, TRAF4, TRAF5, PRKD3, FZD2, ATM, TNFRSF11B, IL8, C1S, IL7, PROZ, TLR2, IL33, PIK3R3, IL1RN, RHOA, GNAO1, FZD6, PIK3CD, MAP2K3, LEF1, FZD5, SFRP1, PDGFD, CAMK2G, ICAM1, FN1, FRZB, PDIA3, NFKBIE, LRP6, CCL5, FZD1, IGHG1, JAK2, C1R, KLK11, CCL2, DKK3, TLR7, CFB, TLR3, TNFRSF1B, ERF, TMPRSS4, SRC, VCAM1, MYD88, WNT2B, PRSS1/PRSS3, GNAQ, NFATC1, IL1R1, PLCB4, CXCL12, WNT11, WNT5A, FZD7, and PRKCB
Dendritic cell maturation	1.20E–08	2.29E–01	MAP2K4, B2M, FCGR3B, ICAM1, NFKBIE, HLA-DQA1, LTB, HLA-DRB1, CD83, HLA-DMB, IGHG1, JAK2, FCGR2B, CD1D, COL1A2, IKBKB, HLA-A, HLA-DRA, HLA-B, LY75, TLR3, CD1C, STAT1, TNFRSF1B, HLA-C, ATM, TNFRSF11B, HLA-DMA, MYD88, FCGR2A, TYROBP, MAPK8, IFNA1/IFNA13, TLR2, IL33, HLA-DQB1, PIK3R3, IL1RN, FCER1G, PIK3CD, IRF8, CCR7, and COL3A1
OX40 signaling pathway	1.45E–08	2.44E–01	B2M, MAP2K4, HLA-DMA, TRAF3, NFKBIE, HLA-DQA1, MAPK8, HLA-DRB1, HLA-DMB, CD3D, HLA-DPA1, HLA-F, HLA-DQB1, HLA-A, HLA-E, HLA-DRA, HLA-B, FCER1G, TRAF5, HLA-G, HLA-DPB1, and HLA-C
Allograft rejection signaling	3.63E–08	2.09E–01	B2M, HLA-DMA, HLA-DQA1, HLA-DRB1, HLA-DMB, IGHG1, FAS, HLA-DPA1, HLA-F, HLA-DQB1, CD28, HLA-A, HLA-E, HLA-DRA, HLA-B, FCER1G, HLA-G, HLA-DPB1, and HLA-C
Graft-versus-host disease signaling	1.41E–06	3.4E–01	HLA-DMA, HLA-DQA1, HLA-DRB1, HLA-DMB, FAS, HLA-F, IL33, HLA-DQB1, CD28, HLA-A, HLA-E, IL1RN, HLA-DRA, HLA-B, FCER1G, HLA-G, and HLA-C
Communication between innate and adaptive immune cells	1.48E–06	2.2E–01	B2M, TLR1, IL8, HLA-DRB1, CD83, CCL5, IGHG1, IFNA1/IFNA13, HLA-F, IL33, TLR2, CD28, HLA-A, HLA-E, IL1RN, HLA-DRA, TLR7, HLA-B, FCER1G, IGHA1, TLR3, HLA-G, CCR7, and HLA-C
Systemic lupus erythematosus signaling	4.37E–06	1.99E–01	FCGR3B, KLK1, CREM, IGHG1, FCGR2B, HLA-F, PTPRC, BDKRB2, CD28, LCK, HLA-A, TLR7, C7, HLA-B, IGL@, IGHM, HLA-G, ATM, HLA-C, FCGR2A, IGKC, NFATC1, CD3D, IFNA1/IFNA13, INPP5D, PIK3R3, IL33, KNG1, IL1RN, HLA-E, FCER1G, LYN, and PIK3CD

Continued on facing page

TABLE 2
Continued

Canonical pathways	*P*	Ratio	Molecules
Caveolar-mediated endocytosis signaling	1.51E–05	2.62E–01	ITGB1, B2M, SRC, ARCN1, ACTB, ITGA2, CD48, EGF, ACTG1, ITGB3, ITGB2, ITGAM, HLA-A, FLNA, RAB5C, PTPN1, CAV1, ITGAV, HLA-B, ITGB6, HLA-C, and ITGA4
B-cell development	1.51E–05	3.51E–01	HLA-DMA, IGKC, HLA-DQA1, HLA-DRB1, HLA-DMB, IGHG1, IL7, IL7R, HLA-DQB1, PTPRC, HLA-DRA, IGL@, and IGHM
Interferon signaling	8.51E–05	3.61E–01	OAS1, JAK1, MX1, IFNGR1, IFI35, IRF9, PSMB8, JAK2, IFNA1/IFNA13, TAP1, IRF1, IFITM1, and STAT1
CTLA4 signaling in CTLs	8.71E–05	2.35E–01	HLA-DMA, AP2B1, AP2M1, PPP2R5C, AP1S2, HLA-DQA1, HLA-DRB1, HLA-DMB, JAK2, AP2A2, CD3D, AP1S1, PIK3R3, HLA-DQB1, CD28, LCK, SYK, HLA-DRA, FCER1G, PIK3CD, PPP2R1B, LCP2, and ATM
CD28 signaling in T-helper cells	9.55E–05	2.12E–01	MAP2K4, ARPC1B, NFKBIE, ARPC5, HLA-DQA1, HLA-DRB1, HLA-DMB, PTPRC, IKBKB, CD28, LCK, ACTR3, HLA-DRA, ARPC3, ATM, HLA-DMA, ACTR2, MAPK8, NFATC1, MALT1, CD3D, HLA-DQB1, PIK3R3, SYK, FCER1G, VAV1, PIK3CD, and LCP2
Integrin signaling	1.23E–04	2.01E–01	MAP2K4, RAP2B, RAC2, ARHGAP26, ARPC1B, ARPC5, NCK1, TSPAN3, ACTR3, CAV1, ITGAV, ARPC3, VCL, ACTN1, ITGA4, ATM, ITGB1, ACTR2, SRC, PAK4, CAPN6, PARVA, PAK2, ACTB, ACTN2, ITGA2, MAPK8, ACTG1, ITGB3, PIK3R3, ITGB2, WIPF1, ITGAM, RND3, ARF3, TSPAN1, MYL12B, RHOA, PPP1R12A, PIK3CD, ITGB6, and FNBP1
Acute-phase response signaling	2.57E–04	2.08E–01	MAP2K4, SERPING1, FN1, APOH, NFKBIE, SERPINA3, JAK2, NR3C1, HRG, HNRNPK, C1R, IKBKB, SOD2, ITIH2, CFB, LBP, TNFRSF1B, TNFRSF11B, C3, MYD88, C1S, MAPK8, SERPINF1, VWF, IL1R1, SERPINF2, IL33, PIK3R3, KLKB1, IL1RN, MAP2K3, PIK3CD, SOCS7, ELK1, SOCS5, A2M, and RBP4
Actin cytoskeleton signaling	3.72E–04	1.76E–01	RAC2, FN1, PFN1, ARPC1B, ARPC5, EGF, ARHGEF1, IQGAP1, SSH1, ACTR3, CYFIP2, BAIAP2, ARPC3, VCL, LBP, MYL10, ACTN1, ITGA4, ATM, ITGB1, ACTR2, PAK4, PAK2, TMSB10/TMSB4X, ACTN2, MYLPF, ACTB, FGF9, ITGA2, ACTG1, PIK3R3, MYL12B, RHOA, ARHGEF6, CD14, PPP1R12A, VAV1, PIK3CD, WASF2, PDGFD, PIP4K2A, and MSN
Role of NFAT in regulation of the immune response	1.07E–03	1.71E–01	BLNK, FCGR3B, NFKBIE, GNB2L1, FCER1A, HLA-DQA1, GNB5, CSNK1A1, HLA-DRB1, HLA-DMB, FCGR2B, GNG7, GNB1, CD28, IKBKB, LCK, HLA-DRA, ATM, HLA-DMA, FCGR2A, GNAQ, NFATC1, CD3D, HLA-DQB1, PIK3R3, PLCB4, SYK, MEF2D, GNAO1, FCER1G, LYN, MEF2C, PIK3CD, and LCP2
Rac signaling	1.10E–03	1.94E–01	MAP2K4, ITGB1, ACTR2, PAK4, PAK2, ARPC1B, ARPC5, ITGA2, MAPK8, IQGAP1, PIK3R3, CYFIP2, ACTR3, RHOA, NCF2, BAIAP2, CD44, CYBB, ARPC3, PIK3CD, ELK1, PIP4K2A, ATM, and ITGA4
Toll-like receptor signaling	1.15E–03	2.55E–01	MAP2K4, TLR1, MYD88, MAPK8, MAP4K4, TLR2, IKBKB, LY96, TLR7, CD14, MAP2K3, TLR3, LBP, and ELK1
Complement system	1.15E–03	3.14E–01	C1R, SERPING1, CD59, C3, C1S, CFB, C7, C1QA, C1QB, CFH, and C3AR1
LXR/RXR activation	1.32E–03	2.04E–01	APOE, MSR1, CD36, APOC2, ARG2, IL1R1, IL33, LY96, CCL2, IL1RN, LPL, CD14, PLTP, LBP, NCOR2, TLR3, TNFRSF1B, RXRA, and TNFRSF11B
Macropinocytosis signaling	1.38E–03	2.37E–01	MRC1/MRC1L1, ITGB1, SRC, EGF, CSF1R, ITGB3, PIK3R3, ITGB2, ABI1, RHOA, HGF, CD14, PIK3CD, ITGB6, PDGFD, PRKD3, PRKCB, and ATM

Continued on next page

TABLE 2
Continued

Canonical pathways	*P*	Ratio	Molecules
Phospholipase C signaling	1.66E–03	1.58E–01	BLNK, GNB2L1, GNB5, HDAC9, ARHGEF1, FCGR2B, GNG7, HDAC6, TGM2, GNB1, LCK, AHNAK, MARCKS, MYL10, ADCY8, PRKD3, ITGA4, ITGB1, SRC, FCGR2A, MYLPF, ITGA2, GNAQ, NFATC1, CD3D, PLA2G4A, PLCB4, RND3, MYL12B, SYK, RHOA, MEF2D, ARHGEF6, FCER1G, LYN, PPP1R12A, MEF2C, ADCY7, FNBP1, LCP2, and PRKCB
Ephrin receptor signaling	1.70E–03	1.71E–01	RAC2, GRIN2A, ARPC1B, GNB2L1, ARPC5, GNB5, EGF, MAP4K4, NCK1, JAK2, GNG7, VEGFA, GNB1, EFNB2, ACTR3, ARPC3, ITGA4, ITGB1, ACTR2, SRC, EPHB4, PAK4, PAK2, CXCR4, ITGA2, GNAQ, EFNA4, WIPF1, ABI1, CXCL12, RHOA, GNAO1, ADAM10, and PDGFD
Death receptor signaling	1.78E–03	2.5E–01	MAP2K4, CASP3, NFKBIE, MAPK8, APAF1, TNFSF10, MAP4K4, FAS, TANK, CASP6, IKBKB, CASP9, CFLAR, CASP8, TNFRSF1B, and BIRC3
Aryl hydrocarbon receptor signaling	2.00E–03	1.76E–01	RARG, SMARCA4, FAS, ARNT, TGM2, MYC, RB1, CTSD, HSP90B1, NR0B2, HSP90AB1, ALDH1A3, TGFB2, AHR, ATM, GSTM1, SRC, APAF1, MAPK8, NCOA3, CYP1B1, CCND2, ALDH1A2, ALDH18A1, NFIB, NCOR2, RXRA, and MCM7
Inhibition of angiogenesis by TSP1	2.09E–03	2.82E–01	MAP2K4, VEGFA, TGFBR2, CD47, SDC1, CASP3, GUCY1A3, THBS1, MAPK8, CD36, and GUCY1B3
Leukocyte extravasation signaling	2.34E–03	1.81E–01	MAP2K4, RAC2, MMP7, ICAM1, CLDN6, TIMP1, CYBB, VCL, PRKD3, ACTN1, ATM, ITGA4, ITGB1, SRC, VCAM1, CXCR4, ACTB, ACTN2, MAPK8, THY1, ACTG1, SELPLG, PIK3R3, ITGB2, WIPF1, ITGAM, CLDN8, CXCL12, RHOA, NCF2, CD44, PECAM1, VAV1, PIK3CD, MSN, and PRKCB
NFκB signaling	2.40E–03	1.83E–01	TLR1, TRAF3, NFKBIE, EGF, MAP4K4, TANK, TGFBR2, IKBKB, LCK, CARD10, UBE2V1, PDGFRA, TLR7, TLR3, TRAF5, CASP8, TNFRSF1B, TNFRSF11B, ATM, MYD88, MAPK8, MALT1, IL1R1, PIK3R3, TLR2, IL33, BMPR1B, IL1RN, NTRK3, FCER1G, PIK3CD, and PRKCB
iCOS-iCOSL signaling in T-helper cells	3.16E–03	1.8E–01	HLA-DMA, NFKBIE, HLA-DQA1, HLA-DRB1, HLA-DMB, NFATC1, CD3D, INPP5D, PIK3R3, HLA-DQB1, PTPRC, CD28, IKBKB, LCK, HLA-DRA, FCER1G, VAV1, PIK3CD, PLEKHA1, LCP2, ATM, and CAMK2G
Fcγ receptor–mediated phagocytosis in macrophages and monocytes	4.07E–03	2.06E–01	ACTR2, SRC, RAC2, ARPC1B, FCGR2A, ACTB, ARPC5, NCK1, FYB, ACTG1, INPP5D, PIK3R3, ACTR3, SYK, LYN, RAB11A, ARPC3, VAV1, PRKD3, LCP2, and PRKCB
CXCR4 signaling	4.17E–03	1.78E–01	MAP2K4, GNB2L1, GNB5, GNG7, GNB1, ADCY8, MYL10, PRKD3, ATM, SRC, PAK4, PAK2, CXCR4, MYLPF, GNAQ, MAPK8, PIK3R3, PLCB4, RND3, MYL12B, RHOA, CXCL12, GNAO1, LYN, PIK3CD, ELMO2, ELK1, ADCY7, FNBP1, and PRKCB
Hepatic fibrosis/hepatic stellate cell activation	4.17E–03	1.97E–01	ICAM1, FN1, EGF, CCL5, FAS, VEGFA, COL1A2, TGFBR2, CCL2, TIMP1, HGF, PDGFRA, TGFB2, LBP, STAT1, TNFRSF1B, TNFRSF11B, IL8, VCAM1, IFNGR1, IL1R1, IFNA1/IFNA13, LY96, IL10RA, EDNRA, CD14, A2M, CCR7, and COL3A1
Interleukin-8 signaling	4.47E–03	1.71E–01	MAP2K4, RAC2, ICAM1, GNB2L1, CXCL1, GNB5, EGF, MAP4K4, GNG7, GNB1, VEGFA, IKBKB, CYBB, PRKD3, TEK, ATM, IL8, SRC, VCAM1, PAK2, MAPK8, CSTB, PIK3R3, ITGB2, CCND2, ITGAM, RND3, MYL12B, RHOA, NCF2, PIK3CD, FNBP1, and PRKCB
Protein kinase Cθ signaling in T lymphocytes	4.90E–03	1.62E–01	MAP2K4, HLA-DMA, RAC2, NFKBIE, HLA-DQA1, MAPK8, HLA-DRB1, HLA-DMB, NFATC1, MALT1, CD3D, PIK3R3, HLA-DQB1, IKBKB, CD28, LCK, HLA-DRA, FCER1G, VAV1, PIK3CD, LCP2, ATM, and CAMK2G

Continued on facing page

TABLE 2
Continued

Canonical pathways	*P*	Ratio	Molecules
TNFR1 signaling	5.37E–03	2.5E–01	MAP2K4, PAK4, PAK2, CASP3, NFKBIE, MAPK8, APAF1, TANK, CASP6, IKBKB, CASP9, CASP8, and BIRC3
PDGF signaling	6.76E–03	2.15E–01	MAP2K4, SRC, JAK1, MAPK8, JAK2, INPP5D, MYC, PIK3R3, SPHK2, PDGFRA, CAV1, PIK3CD, STAT1, PDGFD, ELK1, ATM, and PRKCB
RhoA signaling	6.92E–03	1.86E–01	ACTR2, SEPT8, PFN1, ARPC1B, ACTB, MYLPF, ARPC5, RAPGEF6, ARHGEF1, ACTG1, LPAR6, ACTR3, LPAR1, MYL12B, RHOA, BAIAP2, PPP1R12A, ARPC3, MYL10, PIP4K2A, and MSN
Atherosclerosis signaling	7.76E–03	1.72E–01	IL8, VCAM1, ICAM1, MSR1, CXCR4, CD36, SELPLG, COL1A2, IL33, PLA2G4A, ITGB2, CCL2, IL1RN, CXCL12, LPL, ALOX5, PDGFD, CCR2, ITGA4, and COL3A1
Mitotic roles of polo-like kinase	7.94E–03	2.06E–01	CCNB1, ESPL1, PPP2R5C, CDC20, PRC1, CDC7, CDC25B, HSP90B1, HSP90AB1, PLK2, PPP2R1B, KIF11, and CDC27
Wnt/β-catenin signaling	8.51E–03	1.74E–01	MMP7, WNT10B, FRZB, SOX15, LRP6, CSNK1A1, TLE1, FZD1, RARG, TGFBR2, MYC, SOX9, DKK3, TGFB2, FZD2, SOX4, SRC, PPP2R5C, WNT2B, GNAQ, GNAO1, FZD6, CD44, LEF1, FZD5, SFRP1, PPP2R1B, WNT11, FZD7, and WNT5A
T-helper cell differentiation	9.55E–03	2.08E–01	HLA-DMA, HLA-DQA1, HLA-DRB1, IFNGR1, HLA-DMB, TGFBR2, HLA-DQB1, CD28, HLA-DRA, IL10RB, IL10RA, FCER1G, STAT1, TNFRSF1B, and TNFRSF11B
Sphingosine-1-phosphate signaling	1.00E–02	1.68E–01	CASP3, PDIA3, GNAQ, CASP4, PLCH2, PIK3R3, CASP6, PLCB4, CASP9, RND3, RHOA, CASP1, PDGFRA, PIK3CD, CASP8, PDGFD, ADCY8, ADCY7, FNBP1, and ATM

The results were obtained from Ingenuity Pathway analysis. *P* values were determined using the Fisher exact test, and the ratio was calculated by dividing the number of molecules present in our study by the total molecules in the pathway. The molecules listed are those differentially regulated in our data. CTL, cytotoxic T lymphocyte.

included the antigen-presentation pathway; cytotoxic T lymphocyte–mediated apoptosis; type 1 diabetes signaling; Cdc42; Ras homolog gene family member A (RhoA) signaling; the role of macrophages, fibroblasts, and endothelial cells; dendritic cell maturation; OX40 signaling; allograft rejection; autoimmune thyroid disease; and systemic lupus erythematosus signaling. The list of selected differentially regulated pathways (and the corresponding genes) is shown in Table 2 (and the complete list is in Supplementary Table 6). With the use of the Database for Annotation, Visualization, and Integrated Discovery bioinformatics package, 26 pathways were determined to be statistically significant with a P value < 0.05; the top pathways were again related to type 1 diabetes, viral myocarditis, allograft rejection, graft-versus-host disease, natural killer cell–mediated cytotoxicity, extracellular matrix (ECM) receptor interaction, focal adhesion molecules, and wnt signaling (Supplementary Table 6). Both analyses highlighted the regulation of immune mechanisms and extracellular matrix proteins in the tubulointerstitial compartment of DKD samples.

Pathway analysis in DKD glomeruli. Next, we determined the top differentially regulated pathways in DKD glomeruli using the algorithm detailed earlier. The top pathways with the highest degree of statistical significance were the complement system, RhoA, Cdc42, integrin, integrin-linked kinase (ILK), tight junction, and macropinocytosis (Table 3 and Supplementary Table 6). In addition, semaphorins and vascular endothelial growth factor (VEGF) pathways also showed significant enrichment. Some of these pathways have been proposed to play a role in DKD development.

The Database for Annotation, Visualization, and Integrated Discovery bioinformatics resource (version 6.7) analysis deemed 15 pathways to have statistically significant enrichment in our dataset (Table 3 and Supplementary Table 6). Among these were focal adhesion, ECM receptor interaction, adherens junction, complement and coagulation cascades, the regulation of actin cytoskeleton, as well as Fcγ- and Fcε-mediated signaling pathways (Table 3 and Supplementary Table 6). In summary, our pathway analysis using stringent criteria and two different bioinformatics tools highlighted the regulation of the complement pathway, focal adhesion and integrin, and ECM receptor pathways.

The expression of the complement system in diabetic kidneys. Both the glomerular and tubular analysis identified the complement system as one of the significantly regulated pathways. This was most likely attributed to the fact that complement is absent in control healthy glomeruli, several members of the complement system were differentially expressed in DKD glomeruli (i.e., *C3*, *CD55*, *C1QA*, *CD46*, *C1QB*, *CFB*, *C4A/C4B*, *C7*, *CFH*, *C3AR1*, *CR1*, and *C2*), and all showed a more than threefold change in their expression (Fig. 2 and Table 3). We also detected increased complement expression in the tubulointerstitial compartment of the DKD samples. The relative expression of C3 transcript in individual glomerular samples is graphically represented in Fig. 4*A*. It is important to note that C3 expression was heterogeneous and that most, but not all, cases showed increased *C3* expression.

TABLE 3
Differentially expressed pathways in DKD glomeruli

Canonical pathways	*P*	Ratio	Molecules
Integrin signaling	4.77E–06	2.06E–01	FYN, RAC2, ITGA8, MYLK3, ITGB8, PIK3R4, RHOH, ITGB7, PTEN, PTK2, MYLK, ARF6, ITGAV, AKT3, VCL, ACTN1, ITGB5, PARVA, TSPAN5, PAK2, RRAS, ACTB, CRKL, RAC1, TSPAN2, BCAR3, ITGA3, ITGB3, ROCK1, ITGB2, WIPF1, ITGAM, ARF5, RHOQ, TSPAN1, PLCG2, CAPN1, CAPN2, PIK3CD, ACTN4, TSPAN6, NEDD9, and FNBP1
Complement system	1.96E–05	3.71E–01	CD59, C3, CD55, C1QA, CD46, C1QB, CFB, C4A/C4B, C7, CFH, C3AR1, CR1, and C2
Leukocyte extravasation signaling	8.13E–05	1.91E–01	RAC2, MMP7, NCF1C, CLDN7, MAPK13, RAPGEF4, PIK3R4, RHOH, PTK2, CLDN4, CYBB, MMP11, VCL, PRKD1, ACTN1, TIMP2, TIMP3, MMP28, ACTB, CRKL, RAC1, RDX, RAPGEF3, NCF4, DLC1, ROCK1, BTK, ITGB2, WIPF1, CLDN5, ITGAM, JAM3, ICAM3, PLCG2, CD44, PIK3CD, ACTN4, and CTNND1
Hepatic fibrosis/hepatic stellate cell activation	4.08E–04	2.04E–01	CCR5, CTGF, FN1, LEPR, IL1RL1, CXCR3, CCL5, FAS, VEGFA, COL1A2, TGFBR2, IGF1, HGF, IL1RAP, TIMP2, PDGFRB, SMAD2, VEGFB, FLT1, BAMBI, FGFR2, FGF1, MYL9, COL1A1, KDR, IGFBP3, IL10RA, TGFA, MYH9, and CCR7
Macropinocytosis signaling	1.21E–03	2.24E–01	MRC1/MRC1L1, RRAS, RAC1, ITGB8, PIK3R4, CSF1R, ITGB7, ITGB3, ITGB2, ARF6, ABI1, PLCG2, HGF, PIK3CD, ACTN4, PRKD1, and ITGB5
VDR/RXR activation	1.32E–03	2.35E–01	WT1, IGFBP6, SERPINB1, CYP24A1, SPP1, IL1RL1, KLK6, CCL5, GTF2B, GADD45A, CEBPA, NCOA1, IGFBP3, VDR, IGFBP1, SEMA3B, CDKN1B, CST6, and PRKD1
Glioma invasiveness signaling	2.46E–03	2.33E–01	TIMP3, F2R, RRAS, PIK3R4, RHOH, ITGB3, PTK2, RHOQ, ITGAV, CD44, PIK3CD, ITGB5, FNBP1, and TIMP2
ILK signaling	4.53E–03	1.61E–01	FN1, BMP2, ITGB8, PIK3R4, RHOH, PPP1R14B, ITGB7, PTEN, VEGFA, PTK2, TGFB1I1, PPAP2B, AKT3, ITGB5, ACTN1, MUC1, PARVA, VEGFB, ACTB, FERMT2, VIM, ITGB3, MYL9, ITGB2, RHOQ, PPP2R2B, MYH9, LEF1, PIK3CD, ACTN4, and FNBP1
Germ cell-sertoli cell junction signaling	6.67E–03	1.68E–01	RAC2, LIMK2, IQGAP1, PIK3R4, RHOH, TUBB2B, PTK2, TGFBR2, AGGF1, PPAP2B, MTMR2, ACTN1, PAK2, TJP1, RRAS, ACTB, TUBB2A, RAC1, TUBA4A, ITGA3, RHOQ, TUBB6, PIK3CD, ACTN4, TUBA3C/TUBA3D, FNBP1, CTNND1, and PVRL2
Virus entry via endocytic pathways	8.56E–03	1.8E–01	FYN, RAC2, RRAS, ACTB, CD55, RAC1, ITGB8, ITGA3, PIK3R4, ITGB7, ITGB3, ITGB2, PLCG2, PIK3CD, CXADR, PRKD1, ITGB5, and DNM2
RhoA signaling	1.04E–02	1.68E–01	ARHGEF12, PFN1, ACTB, SEPT7, MYLK3, RDX, CDC42EP3, LIMK2, CDC42EP2, DLC1, MYLK, MYL9, PTK2, ROCK1, LPAR1, IGF1, BAIAP2, SEPT2, and CDC42EP4
Inhibition of angiogenesis by TSP1	1.13E–02	2.31E–01	VEGFA, TGFBR2, FYN, CD47, SDC2, KDR, CD36, AKT3, and MAPK13
Cdc42 signaling	1.20E–02	1.26E–01	PAK2, EXOC1, HLA-DMB, LIMK2, MAPK13, CDC42EP2, IQGAP1, ITGA3, CD3D, APC, HLA-DPA1, HLA-DQB1, MYL9, MYLK, WIPF1, IQGAP2, HLA-DQB2, FNBP1 L, BAIAP2, FCER1G, PARD3, and CLIP1
PTEN signaling	1.23E–02	1.63E–01	RAC2, RRAS, TGFBR3, FLT1, RAC1, FGFR2, ITGA3, INPP5D, PTEN, TGFBR2, PTK2, CSNK2A2, GHR, BMPR1A, KDR, AKT3, PIK3CD, CDKN1B, MAGI2, and PDGFRB
VEGF signaling	1.45E–02	1.72E–01	EIF2S2, VEGFB, RRAS, ACTB, FLT1, PIK3R4, VEGFA, PTK2, ROCK1, PLCG2, KDR, AKT3, PIK3CD, VCL, ACTN4, SFN, and ACTN1

Continued on facing page

TABLE 3
Continued

Canonical pathways	*P*	Ratio	Molecules
Actin cytoskeleton signaling	1.47E–02	1.39E–01	RAC2, PFN1, FN1, F2R, MYLK3, LIMK2, PIK3R4, IQGAP1, MYLK, PTK2, IQGAP2, BAIAP2, DIAPH2, VCL, ACTN1, TIAM1, ARHGEF12, PAK2, RRAS, FGF9, ACTB, CRKL, RAC1, RDX, ITGA3, APC, FGF1, MYL9, ROCK1, CYFIP1, MYH9, PIK3CD, and ACTN4
Role of tissue factor in cancer	1.51E–02	1.75E–01	FYN, CTGF, RRAS, RAC1, HBEGF, LIMK2, MAPK13, PIK3R4, ITGA3, F3, EIF4E, ITGB3, PTEN, VEGFA, LCK, ITGAV, AKT3, PIK3CD, RPS6KA1, and ITGB5
Semaphorin signaling in neurons	1.76E–02	2.12E–01	PTK2, ROCK1, FYN, ARHGEF12, PAK2, RHOQ, DPYSL3, RAC1, LIMK2, RHOH, and FNBP1
Clathrin-mediated endocytosis signaling	1.82E–02	1.52E–01	SH3BP4, RAB4A, EPS15, F2R, SH3GLB1, ITGB8, PIK3R4, ITGB7, VEGFA, ARF6, CD2AP, IGF1, LDLRAP1, DNM2, ITGB5, VEGFB, ACTB, FGF9, RAC1, TSG101, FGF1, ITGB3, ITGB2, CSNK2A2, PIK3CD, and MYO1E
Caveolar-mediated endocytosis signaling	1.88E–02	1.67E–01	FYN, ACTB, ITGA8, CD55, CD48, ITGB8, ITGA3, ITGB7, ITGB3, ITGB2, ITGAM, ITGAV, ITGB5, and DNM2
Lipid antigen presentation by CD1	2.39E–02	2.17E–01	CALR, ARF6, FCER1G, CD1C, and CD1D
Natural killer cell signaling	2.58E–02	1.64E–01	FYN, RAC2, PAK2, LAIR1, TYROBP, RRAS, RAC1, PIK3R4, INPP5D, CD300A, LCK, SH2D1A, SYK, PLCG2, FCER1G, AKT3, PIK3CD, and PRKD1
FcγRIIB signaling in B lymphocytes	3.83E–02	1.53E–01	BLNK, BTK, RRAS, PLCG2, SYK, PIK3CD, FCGR2B, PIK3R4, and INPP5D
Systemic lupus erythematosus signaling	4.11E–02	1.2E–01	CREM, RRAS, IGKC, NFATC1, PIK3R4, FCGR2B, CD3D, FCGR1A, INPP5D, IL33, CD28, LCK, PLCG2, TLR7, FCER1G, C7, IGHM, AKT3, PIK3CD, and FCGR1B
Tight-junction signaling	4.36E–02	1.4E–01	TIAM1, TJP1, ACTB, RAC1, CLDN7, PTEN, TGFBR2, MYL9, MYLK, MPDZ, PRKAR2B, CLDN5, CLDN4, MPP5, JAM3, PPP2R2B, CEBPA, AKT3, MYH9, VCL, SPTAN1, MAGI2, and PVRL2
Primary immunodeficiency signaling	4.41E–02	1.43E–01	IL7R, BLNK, BTK, LCK, IGKC, IGHM, IGHA1, CD8A, and CD3D

The results were obtained from Ingenuity Pathway analysis. *P* value was determined using Fisher exact test, and the ratio was calculated by dividing the number of molecules present in our study by the total molecules in the pathway. The molecules listed are those differentially regulated in our data.

Next, we examined the correlation between C3 transcript and C3 protein expression. C3 immunostaining was performed on the available kidney tissue samples. We found correlation between C3 mRNA and protein expression, as shown in Fig. 4. The correlation coefficient of the semiquantitative immunohistochemistry scoring and the transcript levels were 0.82. Samples that were positive for C3 transcript also showed positive C3 immunostaining (Fig. 4*B*). In summary, we identified complement factor 3 as one differentially expressed transcript in human DKD. C3 transcript and protein expression showed correlation.

We also tested the external validity of the C3 expression in DKD glomeruli by examining 41 additional biopsy-proven DKD cases from our medical center (Table 4). Samples with other concomitant diagnoses (i.e., glomerulonephritis or electron microscope–positive immune complex deposition) were excluded from the analysis. We found that 50% of DKD samples (n = 20) showed positive staining for C3 ranging from 1+ to 3+ (with linear pattern) under fluorescent microscopy, whereas others were negative for C3. Both datasets showed similar, but heterogenous, complement expression. For simplicity, we grouped the cases that had any degree of C3-positive immunostaining together and compared with those that were negative for C3. Clinical and histological data were collected from these patients at baseline to evaluate the correlation between C3 and glomerular injury (Table 4). There was no statistical difference in clinical and renal parameters between the C3-positive and C3-negative groups. From the clinical data, serum albumin levels determined at the time of biopsy were lower in C3-positive cases. Most importantly, we found that the C3-positive cases had a statistically significantly greater percentage of segmental and globally sclerotic glomeruli (49.1 vs. 22.1%). C3-positive cases also were more likely to stain positive for IgG, IgM, κ light chain, λ light chain, and fibrinogen (Table 4). The presence of C3 showed a very strong correlation with the degree of glomerulosclerosis; however, we could not detect statistically significant differences in renal functional parameters between C3-positive and C3-negative cases.

The most examined diabetic kidney samples showed increased expression of C3 mRNA in the tubulointerstitial compartment (Supplementary Fig. S4). However, in contrast to healthy glomeruli, few control (healthy) kidney samples also showed faint C3 expression, mainly in a peritubular (possibly vascular) manner. These observations are consistent with animal-model studies, indicating the expression and the role of tubulointerstitial complement in fibrosis development (22,23).

DISCUSSION

The development of nephropathy in a patient with diabetes is associated with a several-fold increase in mortality. DKD

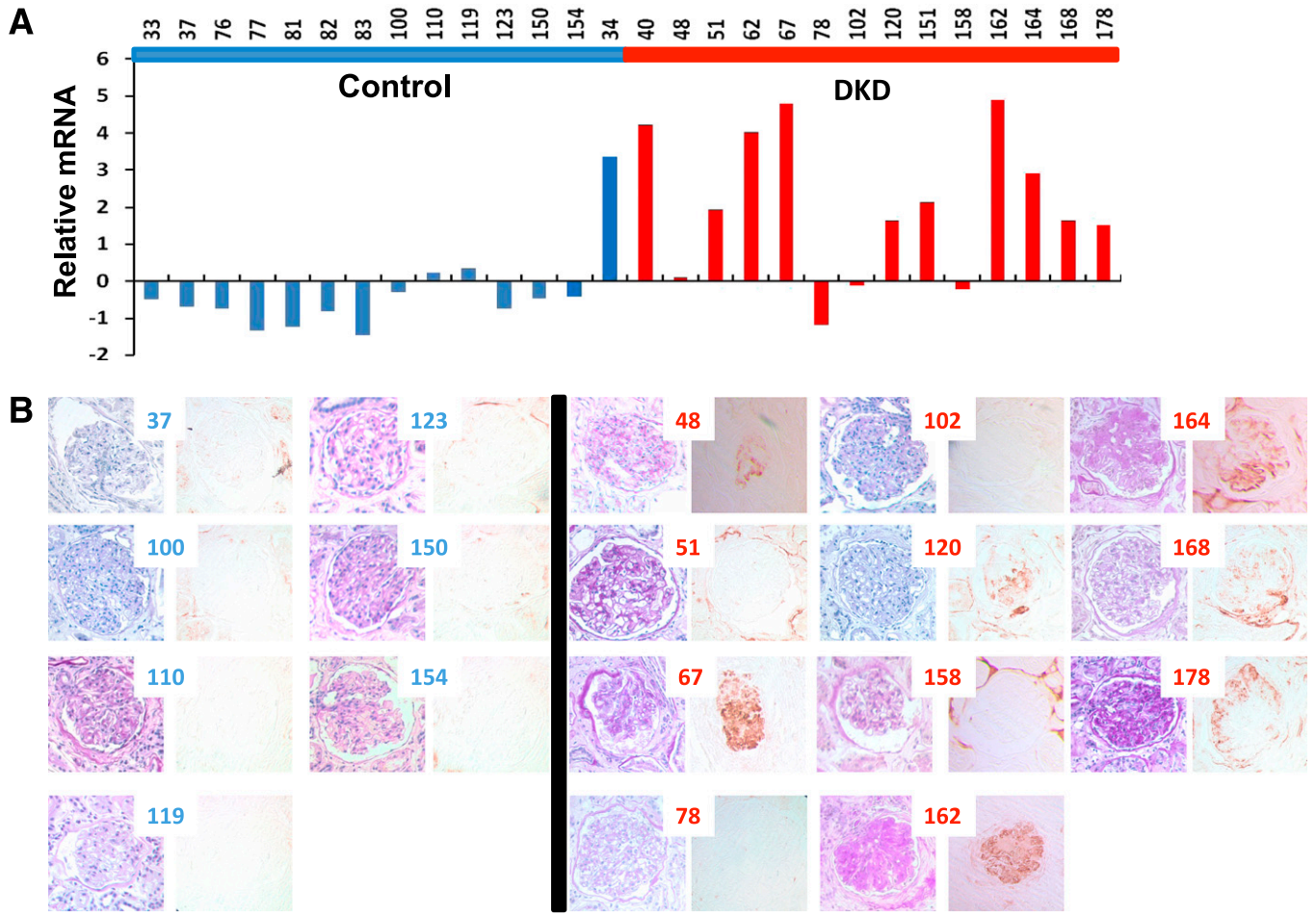

FIG. 4. Increased expression of complement in diabetic glomeruli. *A*: Relative mRNA level of C3 in individual glomerular samples control (blue bars) and from DKD samples (red bars). *B*: Representative images of periodic acid-Schiff staining and C3 immunostaining of individual kidney-tissue samples. (A high-quality digital representation of this figure is available in the online issue.)

remains the number-one cause of end-stage renal disease (ESRD) in the U.S. Because the incidence of diabetes is rising, DKD is recently becoming the primary ESRD cause worldwide. Despite many years of intensive research, genes that would show a strong association to DKD development have not been identified. The understanding of DKD pathomechanism is still elusive, and a cure has not been developed. These issues highlight the importance of using unbiased methodologies for disease understanding.

Previous gene-expression studies performed on mouse models provided important insight into the disease mechanism; however, they are limited as a result of the differences between rodent and human DKD (12). The few human studies that have been performed either used a small sample size (n = 4) (24) or only reported results from the tubulointerstitial compartment (25). Because DKD is a primarily glomerular disease, tubular gene-expression changes may not be relevant to changes that occur in glomeruli. Here, we report the result of a genome-wide transcriptome analysis of an ethnically diverse and larger cohort (n = 44). We believe that our dataset could provide an extremely useful resource for investigators in the field of DKD research because it will enable them to directly query the data and examine the expression and the regulation of individual genes in patients with DKD.

Because glomerular disorders account for the majority of ESRD cases, identification of glomerular-specific transcripts are of key importance. Here, we report the identification of several transcripts with compartmental-specific (glomerular vs. tubulointerstitial) expression. Several previously known glomerular-specific transcripts (*CDKN1*, *PLA2R*, *PLCE1*, *PTPRO*, *NPHS1*, *NPHS2*, and *TCF21*) also were on the top of our list (26). However, several hundred additional transcripts also have been identified by us. Our results indicate that there are not only significant baseline differences (in glomeruli and tubuli), but this difference remains significant in diseased kidneys as well. Our analysis identified only a small number (n = 330 [~18%]) of overlapping probesets that were differentially regulated in both DKD glomeruli and tubuli, and most probesets showed a compartmental-specific regulation.

The unbiased genome-wide approach strongly highlighted the role of podocyte loss in diabetes. Almost all podocyte-specific genes showed a very severe decrease in DKD. The list of genes includes, but is not limited to, *NPHS1*, *NPHS2*, *SYNPO*, *WT1*, *PLCE1*, *PDXL*, *PLA2R1*, and *VEGF*, emphasizing the critical role of podocytes in DKD. The decrease in *NPHS1* (27,28), *NPHS2* (29), *BMP7* (30), *WT1* (31), and *VEGF* (25,32,33) also has been shown in other studies, validating our observations. Decreased podocyte number has been proposed to play a key role in DKD (31).

Our analysis also highlighted the regulation of multiple key pathways, including integrin, ILK, RhoA, Cdc42, and

TABLE 4
Clinical characteristics of additional DKD cases used for the evaluation of C3 expression

	C3 positive	C3 negative	*P*
n	20	21	
Age (years)	52.7 ± 15.36	54.05 ± 11.67	0.752
Sex (female)	14	9	
Race			
Asian Pacific Islander	0	0	
Non-Hispanic white	4	4	
Non-Hispanic black	11	11	
Hispanic	0	3	
Other and unknown	5	3	
Systolic blood pressure (mmHg)	135 ± 25.39	136.33 ± 16.58	0.858
Diastolic blood pressure (mmHg)	76.64 ± 16.52	77.28 ± 10.11	0.894
HbA_{1c}	7.17 ± 1.64	7.81 ± 2.02	0.373
Glucose (mg/dL)	150.61 ± 74.36	188.11 ± 88.62	0.173
Serum C3 level (mg/dL)	118 ± 40.13	133.73 ± 27.96	0.315
Serum albumin (g/dL)	2.82 ± 0.71	3.42 ± 0.56	0.008
Urine protein-creatinine ratio	7.7 ± 0.94	7.8 ± 2.5	0.978
Serum creatinine at biopsy (mg/dL)	2.73 ± 1.73	2.73 ± 1.12	0.994
eGFR (mL/min)	33.35 ± 19.64	32.1 ± 17.28	0.837
Segmentally or globally sclerotic glomeruli (%)	49.1 ± 29.21	22.1 ± 16.1	0.002
Decreased cellularity (%)	42	32	0.223
Increased mesangial matrix (%)	95	100	0.311
Patent lumen (%)	67.67 ± 32.23	73.33 ± 19.7	0.598
IgG	1.9 ± 1.21	0.95 ± 1.12	0.012
IgM	1.74 ± 0.99	0.76 ± 0.83	0.001
IgA	0.47 ± 0.70	0.48 ± 0.81	0.991
C3	1.95 ± 0.83	0	
C1q	0.26 ± 0.65	0.24 ± 0.70	0.907
κ Light chain	1.26 ± 1.19	0.21 ± 0.54	0.001
Λ Light chain	1.11 ± 1.15	0.20 ± 0.52	0.002
Fibrinogen	1.00 ± 1.06	0.25 ± 0.64	0.011

Data are means ± SD unless otherwise indicated. eGFR was calculated using the Modification of Diet in Renal Disease formula. IgG, IgM, IgA, C3, C1q, κ and Λ chain, and fibrinogen are reported on an arbitrary scale of 0–3 (0, normal; 1, mild; 2, moderate; and 3, severe). A Student *t* test was used to determine the statistical significance between groups.

the semaphoring VEGF pathways. Earlier studies described the role of VEGF signaling in DKD development. The activation of the integrin pathway has not been shown using unbiased approaches; however, several studies performed in rodents and in patients have indicated the change in expression of different integrin molecules (34,35). Recent studies indicate that nonenzymatic modification of the different matrix molecules might contribute to integrin activation in DKD (36). On the basis of our results, it would be worthwhile to further examine the role of this pathway in DKD.

Our data emphasize the differential regulation of inflammation and immune-related pathways in both the glomerular and tubular compartments. One of the top differentially regulated pathways in DKD glomeruli and tubuli was the complement system. The presence of C3 has long been noted in human DKD; however, it was thought that C3 is only passively entrapped in diseased glomeruli. We show that transcript levels of C3 and other complement components are increased in DKD glomeruli, indicating that complement may not be "just passively" entrapped in DKD glomeruli but could be locally synthesized. This is further supported by the strong correlation between mRNA and protein expression of C3 in the glomerular compartment. Furthermore, we also confirmed the protein expression of C3 in another group of 38 DKD cases that were not part of the original gene-expression protocol. It is interesting to note that not all DKD samples were C3 positive, and in both of our series 50–60% of the cases expressed C3. C3 positivity could potentially highlight a particular subgroup of DKD patients. In our dataset, the presence of C3 showed a strong correlation with the degree of glomerulosclerosis. However, we could not detect a correlation between C3 positivity and other clinical parameters, including the degree of proteinuria and eGFR. Human genetic studies have implied the importance of the complement system, which may play a role in low-grade inflammation and in the progression of DKD (37). Mechanistic experiments performed on rodent diabetes models also indicated the potential importance of the complement system (38,39). Increased complement expression and activation correlated with DKD severity, whereas complement blockade improved outcomes in different nephropathy models. These results might signify that C3 and the complement system may play a functional role in DKD and glomerulosclerosis. Additional and larger studies may be needed to determine the role and regulation of the complement system in human DKD.

Proteomic studies performed on human kidney tissue samples have not yet been published. Our results, however, show excellent correlation with previous gene-expression and proteomics studies performed on rodent models. We confirmed the regulation of VEGF, connective tissue growth factor (CTGF), and bone morphogenic protein (BMP) 7 in diabetic glomeruli (18,24,40–44). In

addition, similar to other studies, we found increased expression of inflammatory pathways in diabetic tubulointerstitium, which might be related to the regulation of the NFkB pathway (17,45). Proteomics experiments from cultured podocytes indicated the change in expression of ANNEXIN A2 and BMP7, which again correlates with our results (46).

We also need to acknowledge a few inherent limitations of our study. First, this is a single-center study, and for our first analysis we only included subjects with advanced DKD, with both significant sclerosis on histology and significant renal impairment in the clinical parameters. In addition, as in many clinical studies, our results at present are observational in nature because causality cannot be established using this cross-sectional design. Additional studies from our group and other groups might want to focus on earlier disease and a longitudinal design. In addition, although the pathway analysis is a powerful tool to identify differentially regulated pathways, we noted that pathways that we earlier identified as differentially expressed were not represented on the repeat analysis. For example, even though both glomerular and tubular Notch2, glomerular Rbp, and tubule Hey1 transcript levels were statistically significantly increased, the Notch pathway was not among the differentially expressed gene lists. Nevertheless, we believe that this is an important first step to define gene-expression changes in human DKD.

In summary, our study provides the first description of genome-wide gene-expression differences in human DKD glomeruli. Our study highlighted the expression of several known transcripts and pathways previously studied in murine DKD samples and revealed many candidate novel transcripts and pathways that may play important roles in DKD or that could serve as disease biomarkers. Our study could provide a new useful resource for investigators who want to study DKD.

ACKNOWLEDGMENTS

This work was supported by funds from the Juvenile Diabetes Research Foundation and by the National Institutes of Health/National Institute of Diabetes and Digestive and Kidney Diseases (1-R01-DK-087635-01 and R01-DK-076077 to K.S.).

No potential conflicts of interest relevant to this article were reported.

K.I.W. and A.S.D.P. performed the experiments, analyzed the results, and wrote the manuscript. D.M. performed the experiments. D.B.T. and J.M.P. helped with sample collection and evaluation of the histological changes. K.S. designed and supervised the experiments, analyzed the results, and wrote the manuscript.

The authors thank the members of the Montefiore Clinical Pathology Department and the Renal Division for their help with collecting tissue samples.

REFERENCES

1. Foley RN, Collins AJ. End-stage renal disease in the United States: an update from the United States Renal Data System. J Am Soc Nephrol 2007; 18:2644–2648
2. Collins AJ, Foley RN, Gilbertson DT, Chen SC. The state of chronic kidney disease, ESRD, and morbidity and mortality in the first year of dialysis. Clin J Am Soc Nephrol 2009;4(Suppl. 1):S5–S11
3. Tervaert TW, Mooyaart AL, Amann K, et al.; Renal Pathology Society. Pathologic classification of diabetic nephropathy. J Am Soc Nephrol 2010; 21:556–563
4. Xiao X, Ma B, Dong B, et al. Cellular and humoral immune responses in the early stages of diabetic nephropathy in NOD mice. J Autoimmun 2009;32: 85–93
5. KDOQI clinical practice guidelines and clinical practice recommendations for diabetes and chronic kidney disease. Am J Kidney Dis 2007;49(Suppl. 2): S12–S154
6. Perkins BA, Ficociello LH, Ostrander BE, et al. Microalbuminuria and the risk for early progressive renal function decline in type 1 diabetes. J Am Soc Nephrol 2007;18:1353–1361
7. Jones CA, Krolewski AS, Rogus J, Xue JL, Collins A, Warram JH. Epidemic of end-stage renal disease in people with diabetes in the United States population: do we know the cause? Kidney Int 2005;67:1684–1691
8. Iyengar SK, Abboud HE, Goddard KA, et al.; Family Investigation of Nephropathy and Diabetes Research Group. Genome-wide scans for diabetic nephropathy and albuminuria in multiethnic populations: the family investigation of nephropathy and diabetes (FIND). Diabetes 2007;56:1577–1585
9. Schelling JR, Abboud HE, Nicholas SB, et al.; Family Investigation of Nephropathy and Diabetes Research Group. Genome-wide scan for estimated glomerular filtration rate in multi-ethnic diabetic populations: the Family Investigation of Nephropathy and Diabetes (FIND). Diabetes 2008;57: 235–243
10. Brosius FC 3rd, Alpers CE, Bottinger EP, et al.; Animal Models of Diabetic Complications Consortium. Mouse models of diabetic nephropathy. J Am Soc Nephrol 2009;20:2503–2512
11. Susztak K, Sharma K, Schiffer M, McCue P, Ciccone E, Böttinger EP. Genomic strategies for diabetic nephropathy. J Am Soc Nephrol 2003;14 (Suppl. 3):S271–S278
12. Susztak K, Böttinger E, Novetsky A, et al. Molecular profiling of diabetic mouse kidney reveals novel genes linked to glomerular disease. Diabetes 2004;53:784–794
13. Wilson KH, Eckenrode SE, Li QZ, et al. Microarray analysis of gene expression in the kidneys of new- and post-onset diabetic NOD mice. Diabetes 2003;52:2151–2159
14. Schmid H, Boucherot A, Yasuda Y, et al.; European Renal cDNA Bank (ERCB) Consortium. Modular activation of nuclear factor-kappaB transcriptional programs in human diabetic nephropathy. Diabetes 2006;55: 2993–3003
15. Walsh DW, Roxburgh SA, McGettigan P, et al. Co-regulation of Gremlin and Notch signalling in diabetic nephropathy. Biochim Biophys Acta 2008; 1782:10–21
16. Berthier CC, Zhang H, Schin M, et al. Enhanced expression of Janus kinase-signal transducer and activator of transcription pathway members in human diabetic nephropathy. Diabetes 2009;58:469–477
17. Martini S, Eichinger F, Nair V, Kretzler M. Defining human diabetic nephropathy on the molecular level: integration of transcriptomic profiles with biological knowledge. Rev Endocr Metab Disord 2008;9:267–274
18. Baelde HJ, Eikmans M, Lappin DW, et al. Reduction of VEGF-A and CTGF expression in diabetic nephropathy is associated with podocyte loss. Kidney Int 2007;71:637–645
19. Si H, Banga RS, Kapitsinou P, et al. Human and murine kidneys show gender- and species-specific gene expression differences in response to injury. PLoS ONE 2009;4:e4802
20. Ho Sui SJ, Mortimer JR, Arenillas DJ, et al. oPOSSUM: identification of over-represented transcription factor binding sites in co-expressed genes. Nucleic Acids Res 2005;33:3154–3164
21. Huang da W, Sherman BT, Tan Q, et al. DAVID Bioinformatics Resources: expanded annotation database and novel algorithms to better extract biology from large gene lists. Nucleic Acids Res 2007;35:W169–W175
22. Nath KA, Hostetter MK, Hostetter TH. Pathophysiology of chronic tubulointerstitial disease in rats: interactions of dietary acid load, ammonia, and complement component C3. J Clin Invest 1985;76:667–675
23. Correa-Rotter R, Hostetter TH, Nath KA, Manivel JC, Rosenberg ME. Interaction of complement and clusterin in renal injury. J Am Soc Nephrol 1992;3:1172–1179
24. Baelde HJ, Eikmans M, Doran PP, Lappin DW, de Heer E, Bruijn JA. Gene expression profiling in glomeruli from human kidneys with diabetic nephropathy. Am J Kidney Dis 2004;43:636–650
25. Lindenmeyer MT, Kretzler M, Boucherot A, et al. Interstitial vascular rarefaction and reduced VEGF-A expression in human diabetic nephropathy. J Am Soc Nephrol 2007;18:1765–1776
26. Lindenmeyer MT, Eichinger F, Sen K, et al. Systematic analysis of a novel human renal glomerulus-enriched gene expression dataset. PLoS ONE 2010;5:e11545
27. Langham RG, Kelly DJ, Cox AJ, et al. Proteinuria and the expression of the podocyte slit diaphragm protein, nephrin, in diabetic nephropathy: effects of angiotensin converting enzyme inhibition. Diabetologia 2002; 45:1572–1576

28. Doublier S, Salvidio G, Lupia E, et al. Nephrin expression is reduced in human diabetic nephropathy: evidence for a distinct role for glycated albumin and angiotensin II. Diabetes 2003;52:1023–1030
29. Koop K, Eikmans M, Baelde HJ, et al. Expression of podocyte-associated molecules in acquired human kidney diseases. J Am Soc Nephrol 2003;14: 2063–2071
30. Turk T, Leeuwis JW, Gray J, et al. BMP signaling and podocyte markers are decreased in human diabetic nephropathy in association with CTGF overexpression. J Histochem Cytochem 2009;57:623–631
31. Susztak K, Raff AC, Schiffer M, Böttinger EP. Glucose-induced reactive oxygen species cause apoptosis of podocytes and podocyte depletion at the onset of diabetic nephropathy. Diabetes 2006;55:225–233
32. Hohenstein B, Hausknecht B, Boehmer K, Riess R, Brekken RA, Hugo CP. Local VEGF activity but not VEGF expression is tightly regulated during diabetic nephropathy in man. Kidney Int 2006;69:1654–1661
33. Ainsworth SK, Hirsch HZ, Brackett NC Jr, Brissie RM, Williams AV Jr, Hennigar GR. Diabetic glomerulonephropathy: histopathologic, immunofluorescent, and ultrastructural studies of 16 cases. Hum Pathol 1982;13:470–478
34. Jin DK, Fish AJ, Wayner EA, et al. Distribution of integrin subunits in human diabetic kidneys. J Am Soc Nephrol 1996;7:2636–2645
35. Pozzi A, Jarad G, Moeckel GW, et al. Beta1 integrin expression by podocytes is required to maintain glomerular structural integrity. Dev Biol 2008; 316:288–301
36. Pedchenko VK, Chetyrkin SV, Chuang P, et al. Mechanism of perturbation of integrin-mediated cell-matrix interactions by reactive carbonyl compounds and its implication for pathogenesis of diabetic nephropathy. Diabetes 2005; 54:2952–2960
37. Hansen TK, Forsblom C, Saraheimo M, et al.; FinnDiane Study Group. Association between mannose-binding lectin, high-sensitivity C-reactive protein and the progression of diabetic nephropathy in type 1 diabetes. Diabetologia 2010;53:1517–1524
38. Westberg NG, Michael AF. Immunohistopathology of diabetic glomerulosclerosis. Diabetes 1972;21:163–174
39. Colasanti G, Moran J, Bellini A, D'Amico G. Significance of glomerular C3b receptors in human renal diseases. Ren Physiol 1980;3:387–394
40. Thongboonkerd V, Barati MT, McLeish KR, Pierce WM, Epstein PN, Klein JB. Proteomics and diabetic nephropathy. Contrib Nephrol 2004; 141:142–154
41. Sharma K, Lee S, Han S, et al. Two-dimensional fluorescence difference gel electrophoresis analysis of the urine proteome in human diabetic nephropathy. Proteomics 2005;5:2648–2655
42. Barati MT, Merchant ML, Kain AB, Jevans AW, McLeish KR, Klein JB. Proteomic analysis defines altered cellular redox pathways and advanced glycation end-product metabolism in glomeruli of db/db diabetic mice. Am J Physiol Renal Physiol 2007;293:F1157–F1165
43. Zeisberg M, Hanai J, Sugimoto H, et al. BMP-7 counteracts TGF-beta1-induced epithelial-to-mesenchymal transition and reverses chronic renal injury. Nat Med 2003;9:964–968
44. Cummins TD, Barati MT, Coventry SC, Salyer SA, Klein JB, Powell DW. Quantitative mass spectrometry of diabetic kidney tubules identifies GRAP as a novel regulator of TGF-beta signaling. Biochim Biophys Acta 2010; 1804:653–661
45. Starkey JM, Haidacher SJ, LeJeune WS, et al. Diabetes-induced activation of canonical and noncanonical nuclear factor-κB pathways in renal cortex. Diabetes 2006;55:1252–1259
46. Schordan S, Schordan E, Endlich N, et al. Alterations of the podocyte proteome in response to high glucose concentrations. Proteomics 2009;9: 4519–4528